

Electronic Supplementary Information

Highly Parallel Stateful Boolean Logic Gates based on Aluminum-Doped Self-Rectifying Memristors in Vertical Crossbar Array Structure

Taegyun Park,^{a,#} Seung Soo Kim,^{a,#} Byeol Jun Lee,^a Tae Won Park,^a Hae Jin Kim,^{*b} and Cheol Seong Hwang^{*a}

^a *Department of Materials Science and Engineering and Inter-University Semiconductor Research Center, Seoul National University, Seoul 08826, Republic of Korea*

^b *Department of Electronic Materials Engineering, The University of Suwon, Hwaseong-si, Gyeonggi-do, 18323, Republic of Korea*

*E-mail: kimhj@suwon.ac.kr, cheolsh@snu.ac.kr

#These two authors contributed equally to this work.

Supplementary Section I. Self-rectifying memristors in the vertical array structure

The energy dispersive spectrometer (EDS) analysis in Figure S1(a) represents that Al is doped in the HfO_2 region. The resistive switching can occur in the lateral direction between Pt and TiN electrodes.

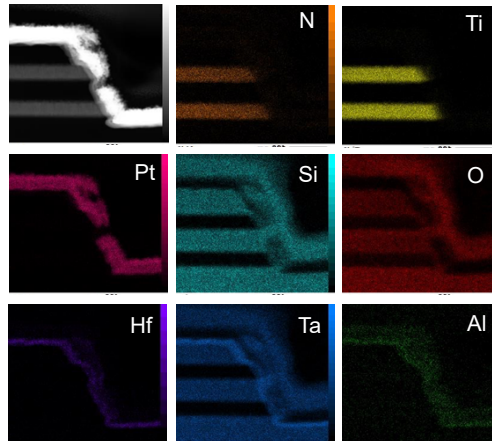


Figure S1. The vertical self-rectifying memristor. The energy dispersive spectrometer composition mapping of the D_{212} memristor.

Supplementary Section II. Parallel logic operations in ASM-two-2AND gates

When the bias of $V_{a,AND}$ is applied to BL1 connecting BL2 to the ground in Fig. 5(a) configuration, four FAS logic gates representing ASM-two-2AND gates can be realized. For each input case, the experimental demonstration is shown in Figure S2.

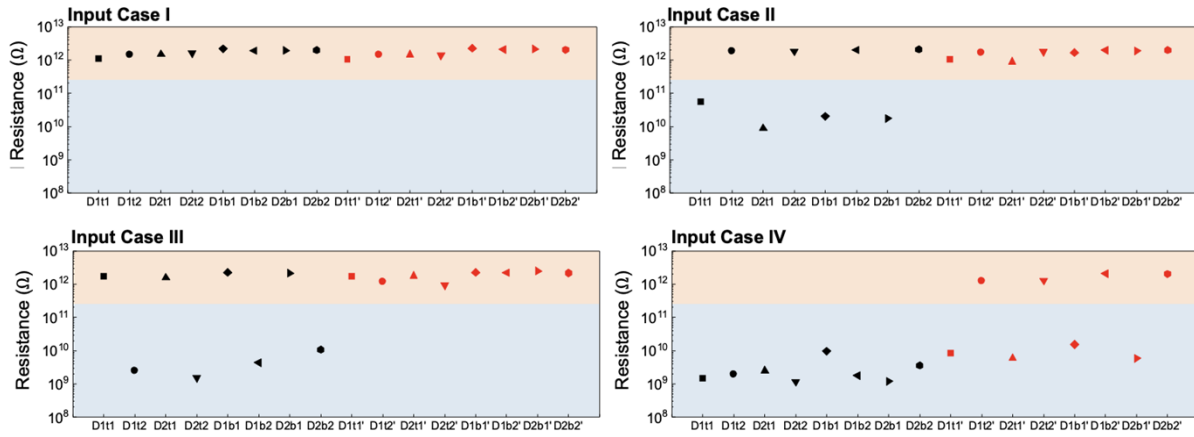


Figure S2. Parallel ASM-two-2AND gates in the two-layered 2×2 vertical crossbar array structure.

Supplementary Section III. Analysis of the sneak current

The sneak current path is formed by the three memristors in parallel to a target memristor in the reading process, as shown in Figure S3. After the logic operation in the ASM-two-2AND gate between D_{1t1} and D_{1t2} , the non-selected memristors (D_{2t1} and D_{2t2}) are switched to R_{on} state while D_{1t2} is assigned for the second input of the logic gate to maximize the sneak current path. Since the equivalent circuit for the sneak path in Figure S3(b) has the reversed memristor, the high forward-reversed rectification ratio can suppress the sneak current in the 2×2 vertical CBA.

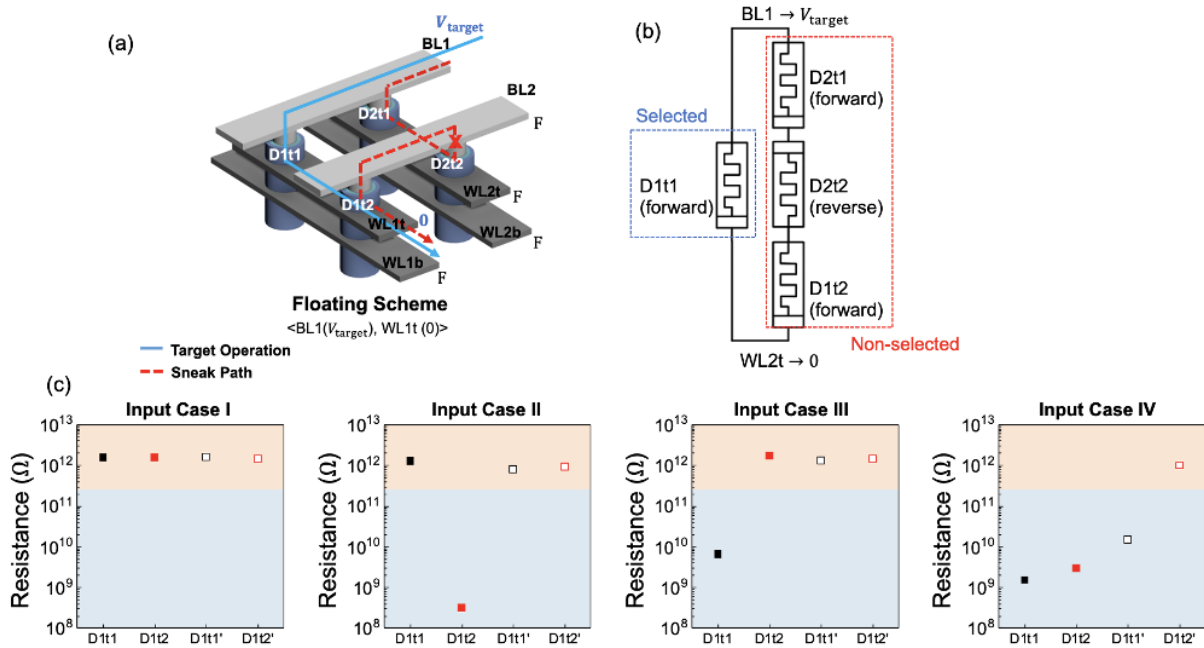


Figure S3. The sneak current paths formed in the 2×2 vertical CBA structure using floating scheme. (a) The schematic diagram of the vertical CBA when bias is applied to D_{1t1} . The sneak current flow to the reversed memristor D_{2t2} is effectively suppressed, indicated by the “x” symbol. (b) The equivalent circuit of the current paths. (c) Experimental demonstration of the ASM-two-2AND gate between D_{1t1} and D_{2t1} when the non-selected memristors, D_{2t1} and D_{2t2} , are initialized to R_{on} .

Supplementary Section IV. Energy band diagram model

In order to construct the energy band diagram model, the simulation model is constructed based on the conduction mechanism of the self-rectifying memristors. The trap level is found to be 1.69 eV measured from the Poole-Frenkel fitting at the high positive voltage in R_{+off} state, as shown in Figure S4-1.

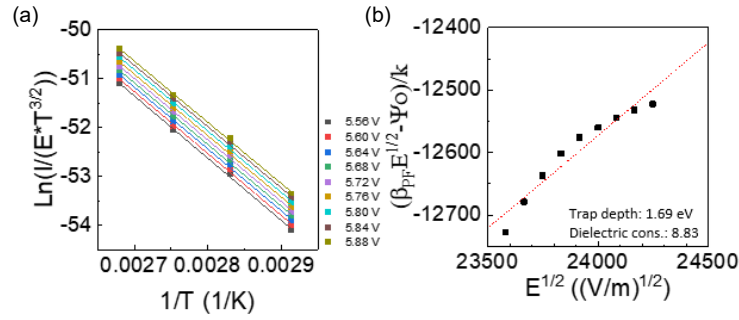


Figure S4-1. Poole-Frenkel fitting of the self-rectifying memristor.

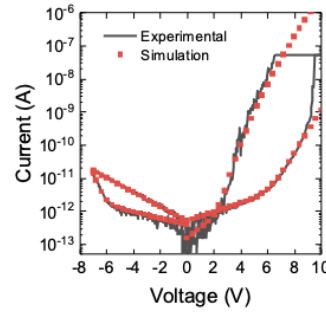


Figure S4-2. Simulation fitting model of the self-rectifying memristors.

The simulation model based on the experimental results can be constructed to calculate the applied bias to the memristor in the two anti-serial memristors using Verilog-A model, as shown in Figure S4-2. Accordingly, the voltage drops over each memristor for ASM-two-2AND and ASM-two-2OR gates can be simulated, as shown in Table S4-1. Then, the electric field applied to HfO_2 and Ta_2O_5 can be found from the boundary equations.

Table S4-1. The voltage drops over each memristor when the conditional bias for the logic gates is applied.

ASM-two-2AND	V_{D111} [V]	V_{D112} [V]	ASM-two-2OR	V_{D111} [V]	V_{D211} [V]
Input case I	3.503	5.497	Input case I	6.351	5.650
Input case II	5.394	3.606	Input case II	7.852	4.148
Input case III	2.705	6.295	Input case III	5.459	6.541
Input case IV	3.103	5.897	Input case IV	8.430	3.570

1) Considering the work functions of Pt and TiN, the sum of the voltage across HfO_2 and Ta_2O_5 equals to applied voltage.

$$V_a = V_{\text{HfO}_2} + V_{\text{Ta}_2\text{O}_5} = d_{\text{HfO}_2} E_{\text{HfO}_2} + d_{\text{Ta}_2\text{O}_5} E_{\text{Ta}_2\text{O}_5} + \phi_{\text{Pt}} - \phi_{\text{TiN}} \quad (\text{S4-1})$$

2) Electric flux is assumed to be constant that there is no surface charge at the interface between HfO_2 and Ta_2O_5 .

$$D_{\text{HfO}_2} = D_{\text{Ta}_2\text{O}_5}, \quad E_{\text{HfO}_2} \epsilon_{\text{HfO}_2} = E_{\text{Ta}_2\text{O}_5} \epsilon_{\text{Ta}_2\text{O}_5} \quad (\text{S4-2})$$

Solving the two equations yield the electric field applied to HfO_2 and Ta_2O_5 .

$$d_{\text{HfO}_2} E_{\text{HfO}_2} + d_{\text{Ta}_2\text{O}_5} E_{\text{Ta}_2\text{O}_5} = V_a - (\phi_{\text{Pt}} - \phi_{\text{TiN}}) \quad (\text{S4-3})$$

$$-\varepsilon_{\text{HfO}_2} E_{\text{HfO}_2} + \varepsilon_{\text{Ta}_2\text{O}_5} E_{\text{Ta}_2\text{O}_5} = 0 \quad (\text{S4-4})$$

$$\begin{bmatrix} d_{\text{HfO}_2} & d_{\text{Ta}_2\text{O}_5} \\ -\varepsilon_{\text{HfO}_2} & \varepsilon_{\text{Ta}_2\text{O}_5} \end{bmatrix} \begin{bmatrix} E_{\text{HfO}_2} \\ E_{\text{Ta}_2\text{O}_5} \end{bmatrix} = [V_a - (\phi_{\text{Pt}} - \phi_{\text{TiN}})] \begin{bmatrix} 1 \\ 0 \end{bmatrix} \quad (\text{S4-5})$$

$$\begin{aligned} \begin{bmatrix} E_{\text{HfO}_2} \\ E_{\text{Ta}_2\text{O}_5} \end{bmatrix} &= \frac{V_a - (\phi_{\text{Pt}} - \phi_{\text{TiN}})}{\varepsilon_{\text{Ta}_2\text{O}_5} d_{\text{HfO}_2} + \varepsilon_{\text{HfO}_2} d_{\text{Ta}_2\text{O}_5}} \begin{bmatrix} \varepsilon_{\text{Ta}_2\text{O}_5} & -d_{\text{Ta}_2\text{O}_5} \\ \varepsilon_{\text{HfO}_2} & d_{\text{HfO}_2} \end{bmatrix} \begin{bmatrix} 1 \\ 0 \end{bmatrix} \\ &= \frac{V_a - (\phi_{\text{Pt}} - \phi_{\text{TiN}})}{\frac{\varepsilon_{\text{Ta}_2\text{O}_5} \varepsilon_{\text{HfO}_2}}{d_{\text{Ta}_2\text{O}_5} + \frac{\varepsilon_{\text{HfO}_2}}{d_{\text{HfO}_2}}}} \begin{bmatrix} \varepsilon_{\text{Ta}_2\text{O}_5} & -d_{\text{Ta}_2\text{O}_5} \\ \varepsilon_{\text{HfO}_2} & d_{\text{HfO}_2} \end{bmatrix} \begin{bmatrix} 1 \\ 0 \end{bmatrix} \end{aligned} \quad (\text{S4-6})$$

$$E_{\text{HfO}_2} = \frac{V_a - (\phi_{\text{Pt}} - \phi_{\text{TiN}})}{\frac{\varepsilon_{\text{HfO}_2}}{d_{\text{Ta}_2\text{O}_5} + \frac{\varepsilon_{\text{HfO}_2}}{d_{\text{HfO}_2}}}}, \quad E_{\text{Ta}_2\text{O}_5} = \frac{V_a - (\phi_{\text{Pt}} - \phi_{\text{TiN}})}{\frac{\varepsilon_{\text{Ta}_2\text{O}_5}}{d_{\text{Ta}_2\text{O}_5} + \frac{\varepsilon_{\text{HfO}_2}}{d_{\text{HfO}_2}}}} \quad (\text{S4-7})$$

As a result, the band diagram can be drawn using the electric field and material parameters from the reference in Table S4-2.

Table S4-2. Summarized material parameters for Ta₂O₅, HfO₂, Pt, and TiN used in the energy band diagram model.

Material Parameters	
$\chi_{\text{Ta}_2\text{O}_5}$	3.2 eV
χ_{HfO_2}	2.2 eV
ϕ_{TiN}	4.52 eV
ϕ_{Pt}	5.65 eV
$d_{\text{Ta}_2\text{O}_5}$	5 nm
d_{HfO_2}	10 nm
$E_{\text{g,Ta}_2\text{O}_5}$	4.4 eV
$E_{\text{g,HfO}_2}$	5.7 eV